We are IntechOpen,
the world's leading publisher of
Open Access books
Built by scientists, for scientists

6,900
Open access books available

185,000
International authors and editors

200M
Downloads

Our authors are among the

154
Countries delivered to

TOP 1%
most cited scientists

12.2%
Contributors from top 500 universities

BOOK CITATION INDEX
CLARIVATE ANALYTICS
INDEXED

WEB OF SCIENCE™

Selection of our books indexed in the Book Citation Index
in Web of Science™ Core Collection (BKCI)

Interested in publishing with us?
Contact book.department@intechopen.com

Numbers displayed above are based on latest data collected.
For more information visit www.intechopen.com

DTC-SVM Approaches of an Induction Motor Dedicated to Position Control Applications

Fatma Ben Salem

Abstract

The chapter is devoted to the DTC and DTC-SVM position control approaches of induction motor (IM) allowing the movement of a photovoltaic panel according to the maximum sunshine position to extract a high efficiency of the system. The DTC is selected to full the application requirements, especially a maximum torque at standstill. This feature is necessary in order to guarantee a high degree of robustness of the maximum sunshine position tracking system against the high and sudden load torque variations characterized by the gusts of wind. The first step is devoted to a comparison study between three DTC strategies, dedicated to position control, such that: the basic DTC strategy, the DTC strategy with a look-up table including only active voltage vectors, and the DTC-SVM strategy with hysteresis controllers. Furthermore, the synthesis and the implementation of DTC-SVM approaches based on position control are treated. Within this context, the final part of the chapter proposes a comparison between three DTC-SVM approaches: (i) a DTC-SVM approach using PI controllers, (ii) a DTC-SVM approach using PI controllers with a nonlinear compensator, and (iii) a DTC-SVM approach using sliding mode controllers. In that case, an adaptation approach of parameter estimators are implemented in order to eliminate the effects of parameter variations and load disturbances. Simulations results show that the SM DTC-SVM approach gives the best results.

Keywords: induction machine, position control, SM, DTC, SVM, parameters variations, load disturbances

1. Introduction

Induction motors (IM) are very common because they are inexpensive and robust, finding use in everything from industrial applications such as pumps, fans, and blowers to home appliances. In recent years, the control of high-performance IM drives for general industrial applications and production areas has received a lot of research interests.

The most modern technique, for the induction machine, is the direct torque and the stator flux vector control method (DTC). It has been realized in an industrial way by ABB, using the theoretical background proposed by *Takahashi* [1] and Depenbrock [2] in the middle of 1980's. Over the years, DTC method becomes one of the high-performance control strategies for AC machines to provide a very fast torque and flux control [3, 4].

The DTC has been selected in order to fulfill the application requirements, especially a maximum torque at standstill. This feature is necessary in order to guarantee a high degree of robustness of the maximum sunshine position tracking system against the high and sudden load torque variations characterized by the gusts of wind. This positioning system can be introduced in the multi-sources hybrid system, in order to allow high efficiencies of photovoltaic systems. To do so, an electric motor drive could be associated with photovoltaic panels in order to be able to track the maximum sunshine positions during the day. In what follows, the chapter will be focused on the problem of position regulation of an induction motor under DTC and DTC-SVM strategies.

2. A case study: solar panel positioning

2.1 Problem heading

Photovoltaic panels are commonly exposed to the sun in a fixed position corresponding to the maximum sunshine recorded during a day that is the position of the sun at midday. Nevertheless, this strategy does not allow the extraction of the maximum power during a day and therefore a high efficiency of photovoltaic systems, which can be integrated with the multi-source hybrid system, described above. An approach to solve this problem consists in moving photovoltaic panels according to the maximum sunshine position. To do so, an electric motor drive could be associated with photovoltaic panels in order to be able to track the maximum sunshine positions during the day. Accounting for the high perturbation amplitude applied to the panel, the control strategy to be implemented in the drive is of great importance [5].

The proposed tracking system has two freedom degrees in such a way that it allows the displacement of the photovoltaic system within latitudes and meridians: the first degree of freedom is controlled automatically by an IM drive under the control of a DTC strategy.

The DTC approach has been selected in order to full the application requirements, especially a maximum torque at standstill. This feature is necessary in order to guarantee a high degree of robustness of the maximum sunshine position tracking system against the high and sudden load torque variations characterized by the gusts of wind.

The following work will be focused on the study of the first freedom degree. Special attention is paid to the implementation of a suitable DTC strategy in the IM drive.

2.2 Mathematical model of induction machines

The dynamic behavior of an induction machine is defined in terms of space variables in the sequel:

$$
\begin{cases}
\dfrac{d}{dt}\phi_{\alpha s} = v_{\alpha s} - R_s i_{\alpha s} \\[2mm]
\dfrac{d}{dt}\phi_{\beta s} = v_{\beta s} - R_s i_{\beta s} \\[2mm]
\dfrac{d}{dt}\phi_{\alpha r} = -R_r i_{\alpha r} - \omega_m \phi_{\beta r} \\[2mm]
\dfrac{d}{dt}\phi_{\beta r} = -R_r i_{\beta r} + \omega_m \phi_{\alpha r}
\end{cases}
\tag{1}
$$

considering that subscripts s and r refer to stator and rotor, subscripts α and β refer to components in (α, β) frame, v, i and φ refer to voltage, current and flux, R_s and R_r refer to stator and rotor resistances, and ω_m refers to the machine speed ($\omega_m = N_p\Omega_m = \omega_s - \omega_r$ and N_p is the pole pair number).

Relationships between currents and flux are:

$$\begin{cases} \phi_{\alpha s} = L_s i_{\alpha s} + M i_{\alpha r} \\ \phi_{\alpha r} = M i_{\alpha s} + L_r i_{\alpha r} \\ \phi_{\beta r} = M i_{\beta s} + L_r i_{\beta r} \\ \phi_{\beta s} = L_s i_{\beta s} + M i_{\beta r} \end{cases} \quad (2)$$

where L and M refer to the inductance and the mutual one.

The mechanical part of the machine is described by:

$$J\frac{d}{dt}\Omega_m = T_{em} - T_l \quad (3)$$

where J is the motor inertia and T_l represent the load torque.

2.3 Voltage source inverter

The made constant DC voltage by the rectifier is delivered to the inverter input, which thanks to controlled transistor switches, converts this voltage to three-phase AC voltage signal with wide range variable voltage amplitude and frequency.

The voltage vector of the three-phase voltage inverter can be represented as follows:

$$\vec{V}_s = \sqrt{\frac{2}{3}}\left[S_a + S_b e^{j\frac{2\pi}{3}} + S_c e^{j\frac{4\pi}{3}}\right] \quad (4)$$

where S_a, S_b and S_c are three-phase inverter switching functions, which can take a logical value of either 0 or 1.

2.4 Basic concept of DTC based position control

The implementation scheme of the *Takahashi* basic DTC strategy applied to the position regulation of an induction motor drive is shown in **Figure 1**.

Referring to [5, 6], it has been found that the *Takahashi* basic DTC strategy is penalized at low speeds by the so-called "demagnetization phenomenon" which is caused by the systematic application of zero voltage vectors when the torque regulator output is zero, independently of the flux regulator output state. Indeed, the application of these voltage vectors during a sampling period T_s yields a slight decrease of the stator flux at high speeds. However, at low speeds, the application of zero voltage vectors leads to a high reduction of the stator flux, yielding the demagnetization problem which affects the electromagnetic torque.

In order to overcome this shortcoming, the zero-voltage vectors can be substituted by active ones. For a given stator flux vector and when the torque regulator output is "0", the active vector around which is located the sector including the stator flux vector, is applied. The resulting look-up table is given in **Table 1**. Nevertheless, this substitution is associated to an other crucial problem: that is an increase of the inverter switching frequency which compromises the drive efficiency.
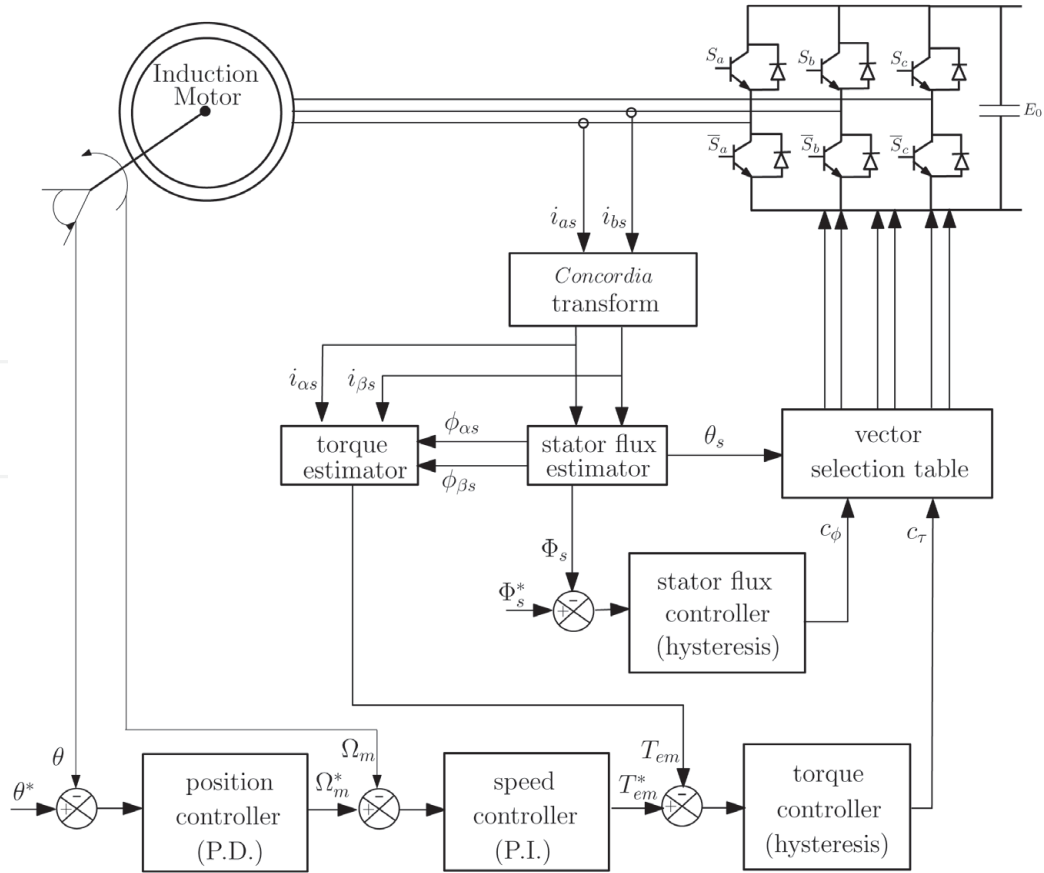
Figure 1.
IM position regulation based on basic DTC strategy.

c_ϕ	+1			−1		
c_r	+1	0	−1	+1	0	−1
S1	V_2 (100)	V_1 (101)	V_6 (001)	V_3 (110)	V_4 (010)	V_5 (011)
S2	V_3 (110)	V_2 (100)	V_1 (101)	V_4 (010)	V_5 (011)	V_6 (001)
S4	V_4 (010)	V_3 (110)	V_2 (100)	V_5 (011)	V_6 (001)	V_1 (101)
S4	V_5 (011)	V_4 (010)	V_3 (110)	V_6 (001)	V_1 (101)	V_2 (100)
S5	V_6 (001)	V_5 (011)	V_4 (010)	V_1 (101)	V_2 (100)	V_3 (110)
S6	V_1 (101)	V_6 (001)	V_5 (011)	V_2 (100)	V_3 (110)	V_4 (010)

Table 1.
*Look-up table with zero-voltage vectors substituted by active ones.*

2.5 Concept of DTC-SVM with hysteresis controllers based position control

The implementation scheme of the DTC-SVM strategy with hysteresis control-lers applied to the position regulation of an induction motor drive is shown in **Figure 2**. It has the same layout as the one of the basic DTC strategy proposed in section II, except that the SVM bloc is added to the control system that ensures an imposed switching frequency [7–12].

2.6 Simulations and discussions: A comparative study

The ratings and parameters of the induction machine, used in the simulation study, are listed in **Tables 2** and **3** respectively.

- The sampling period T_s has been chosen equal to $50\mu s$ in the cases of the first and the second strategies, whereas in the case of the third strategy, it has been chosen equal to $100\mu s$.

- Bandwidths of flux and torque hysteresis regulators have been chosen as: $\varepsilon_\phi = 0.02\,Wb$ and $\varepsilon_\tau = 5N$ for the two first strategies, whereas for the third one, they have been selected as $\varepsilon_\phi = 0.02\,Wb$ and $\varepsilon_\tau = 3.5N$.

- The load torque is given by the following expression: $T_l = K \sin\theta$. K has been calculated and has been found equal to 57.762 N.m.

- The modulation period has been fixed to $T_{mod} = 150\mu s$ in DTC-SVM approach under study.
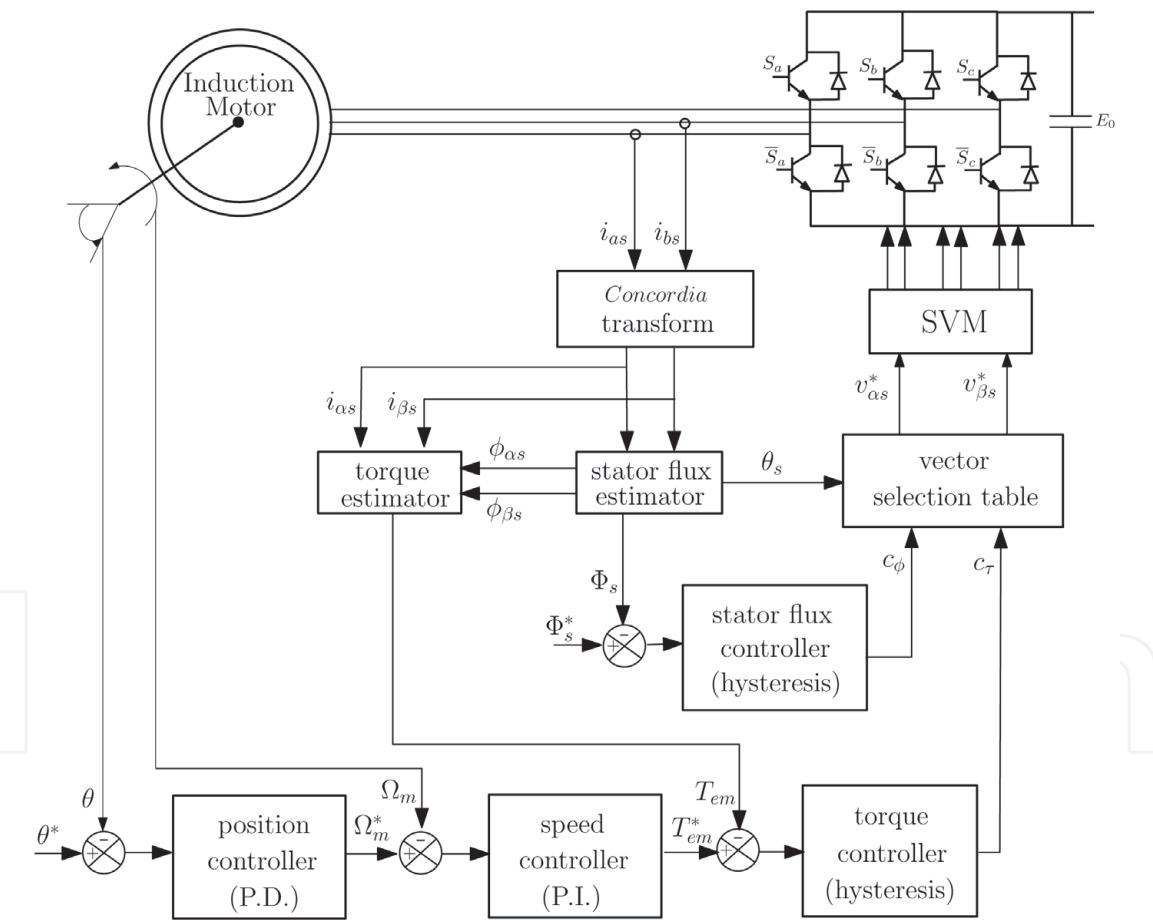
Figure 2.
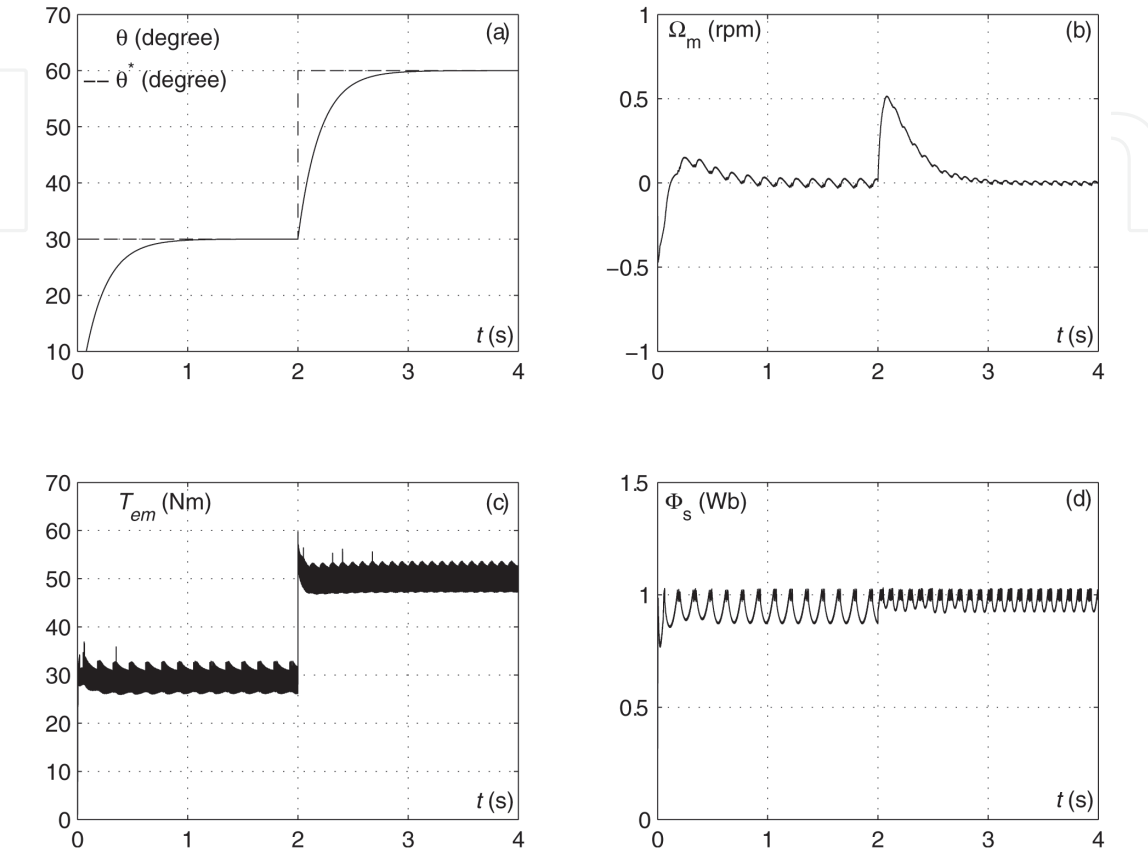*Induction motor position regulation based on the DTC-SVM strategy.*

Power	10 kW	Voltage	380 V/220 V
Efficiency	80%	Current	24A/41A
Speed	1500 rpm	Frequency	50 Hz

Table 2.
Induction machine ratings.

| $r_s = 0.29\Omega$	$r_r = 0.38\Omega$	$M = 47.3\text{mH}$
$L_s = L_r = 50\text{mH}$	$N_p = 2$	$J = 0.5\text{Kg.m}^2$

Table 3.
Induction machine parameters.
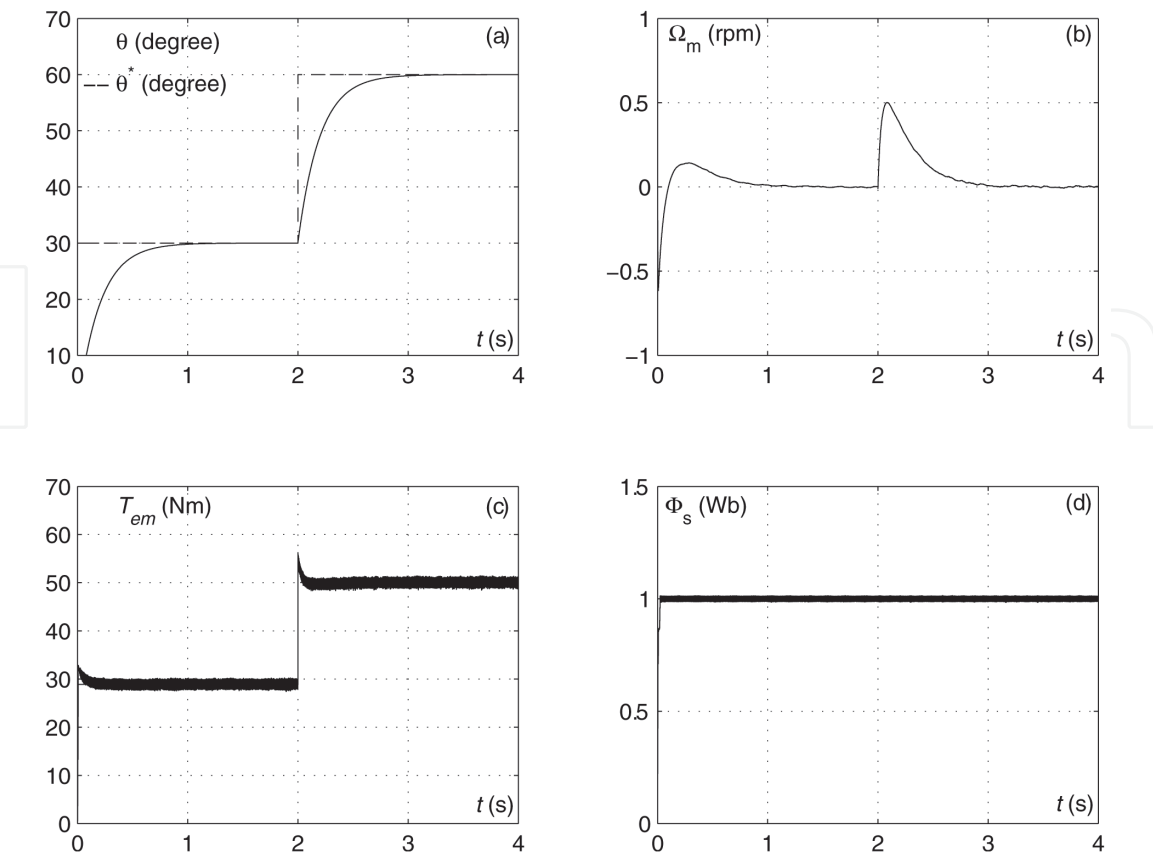

Figure 3.
Induction motor position regulation under the basic Takahashi DTC strategy, (a): Rotor position θ and its reference, (b): Speed Ω_m, (c): Electromagnetic torque T_{em}, (d): Stator flux Φ_s.

Figures 3–5 show the induction motor dynamic following the application of a dual-step reference position under the basic *Takahashi* DTC strategy, the modified *Takahashi* one, and the DTC-SVM strategy with a controlled commutation frequency, respectively. In order to highlight performances gained by the DTC-SVM scheme, resulting features are compared to the obtained ones following the implementation of the basic DTC strategy. The analysis of these results leads to the following remarks:

- **Figures 3a–5a** show that the three DTC strategies exhibit almost the same position and speed dynamics,

- Performances of the flux loop of the basic *Takahashi* DTC strategy is affected by the demagnetized phenomenon (**Figure 3d**). In fact, the analysis of the *Takahashi* strategy highlights low performances at low speed operations. Under such conditions, and for steady state operations, the motor turns to be demagnetized.

- In order to overcome the demagnetization problem caused by zero-voltage vectors included in the look-up table of the basic DTC strategy, these have
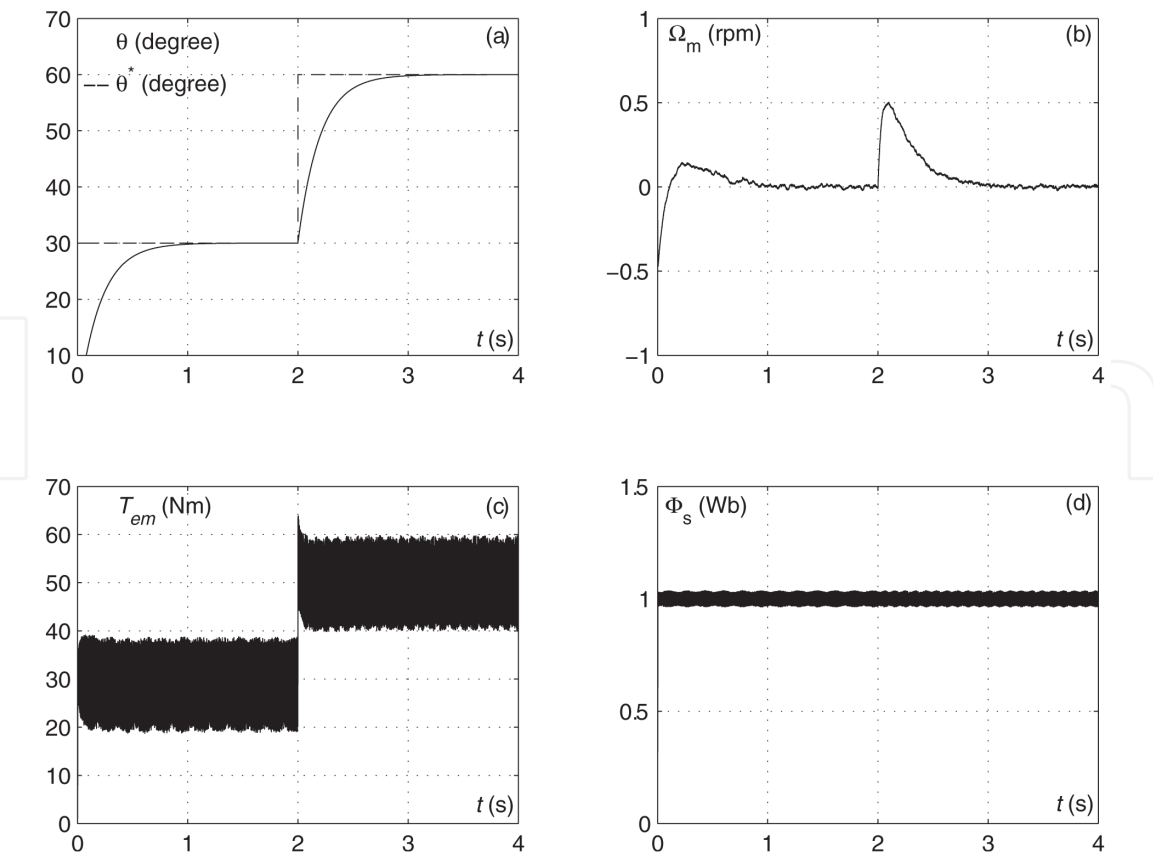
Figure 4.
Induction motor position regulation under the modified Takahashi DTC strategy, (a): Rotor position θ and its reference, (b): Speed Ω_m, (c): Electromagnetic torque T_{em}, (d): Stator flux Φ_s.
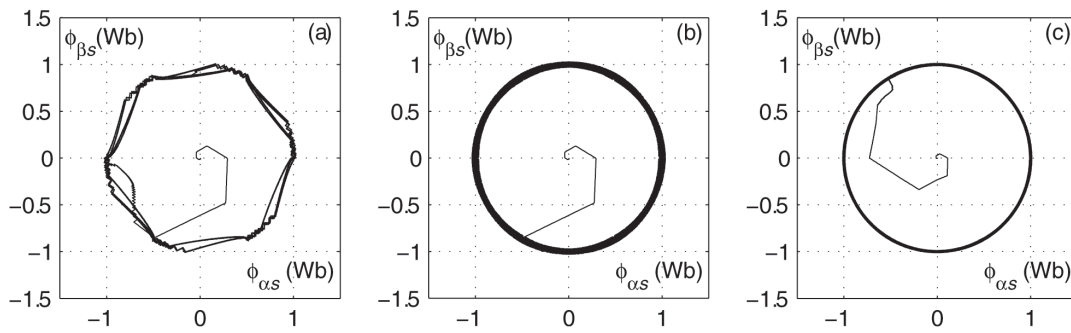

Figure 5.
Induction motor position regulation under the DTC-SVM strategy with a constant commutation frequency of 6.5 kHz, (a) rotor position θ, (b): Speed Ω_m; (b): Electromagnetic torque T_{em}, (d): Stator flux Φ_s.

been substituted by active vectors. Obtained results are illustrated in **Figure 4**. Referring to **Figure 4d**, one can notice that the demagnetization problem has been removed, while performances of the motor, for high speeds, are not affected. However, the torque ripple amplitudes rise considerably (**Figure 4c**) with respect to the one yielded by the *Takahashi* DTC strategy, which represents a severe drawback.

- **Figure 5** shows that the DTC-SVM strategy exhibits high dynamical performances. In fact, this approach presents a low torque ripple amplitude (**Figure 5c**). Moreover, it completely eliminates the demagnetization phenomenon (**Figure 5d**).

Further investigation of the stator flux has been achieved through the represen-tation of the stator flux vector extremity locus in the $(\alpha, \ \beta)$ plane. This has been

Figure 6.
Locus of the extremities of $\overline{\Phi}_s$, with (a) basic Takahashi DTC strategy, (b) modified Takahashi DTC strategy and (c) DTC-SVM strategy with a constant commutation frequency.
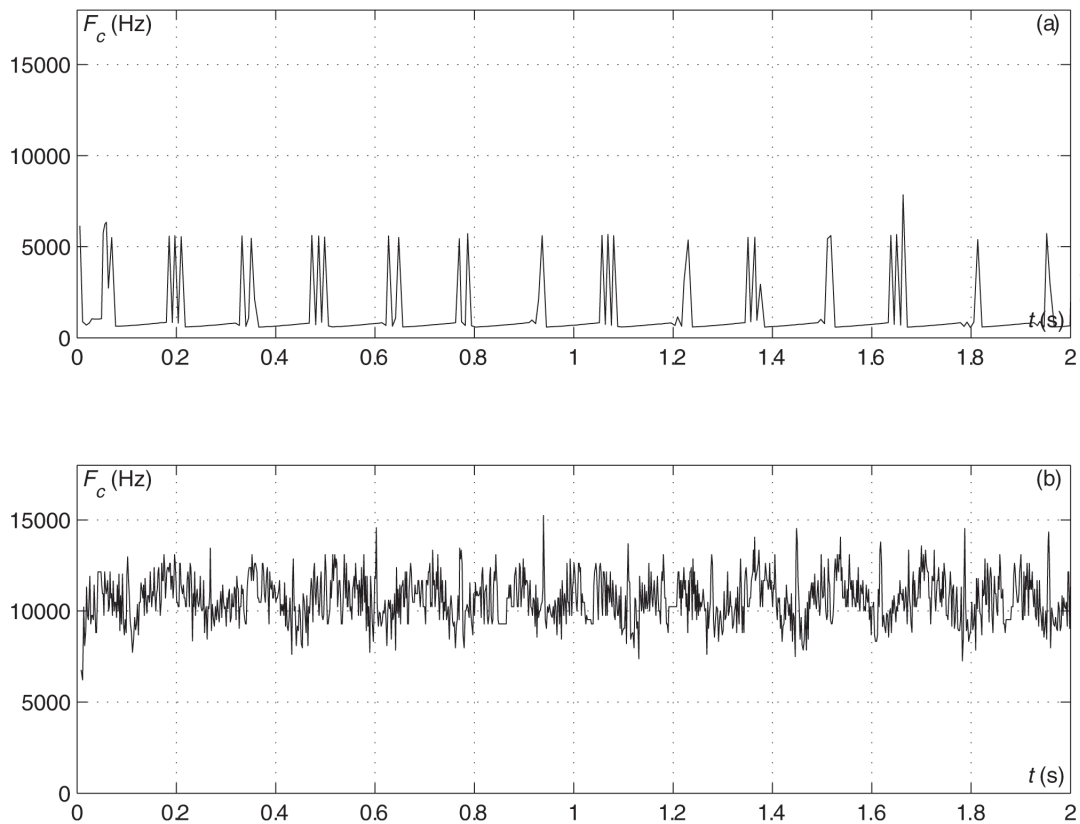
Figure 7.
Average commutation frequency of the inverter power switches, (a) basic Takahashi DTC strategy, (b) modified Takahashi DTC strategy.

done considering the three DTC strategies. Obtained results are shown in **Figure 6**. One can notice, easily, that the DTC-SVM strategy with hysteresis regulators and with an imposed commutation frequency yields to the smoothest circular locus.

Finally, we have involved in the assessment of the average commutation frequencies of both basic and modified *Takahashi* DTC strategies. Obtained results have been showing in **Figure 7**. It is to be noted that the basic DTC strategy and the DTC-SVM with an imposed commutation frequency ($F_c = 6.25kHz$) strategy offer lower commutation frequencies than the modified *Takahashi* DTC strategy.

3. Concept of PI DTC-SVM based position control

3.1 Computing of flux reference coordinates

The slip angular reference speed ω_r^*, which is the output of the PI controller, will be used to calculate the argument of the stator flux reference. In the reference frame $(\alpha, \ \beta)$, coordinates of the reference stator flux $\phi_{\alpha s}^*$ and $\phi_{\beta s}^*$ are calculated from the polar coordinates according to the following expressions:

$$\begin{cases} \phi_{\alpha s}^* = |\Phi_s^*| \cos \theta_s^* \\ \\ \phi_{\beta s}^* = |\Phi_s^*| \sin \theta_s^* \end{cases} \tag{5}$$

3.2 Computing of voltage reference coordinates

The coordinates of references of voltage vectors $v_{\alpha s}^*$ and $v_{\beta s}^*$ in $(\alpha, \ \beta)$ frame are determined by the following equations:

$$\begin{cases} V_{\alpha s}^* = \dfrac{\phi_{\alpha s}^* - \phi_{\alpha s}}{T_e} + R_s i_{\alpha s} \\ \\ V_{\beta s}^* = \dfrac{\phi_{\beta s}^* - \phi_{\beta s}}{T_e} + R_s i_{\beta s} \end{cases} \tag{6}$$

Finally, they are introduced to the SVM block, which uses them to control the inverter switches (S_a, S_b, S_c).

3.3 Position control loop

The objective is the design of a suitable controller as described by **Figure 8**.
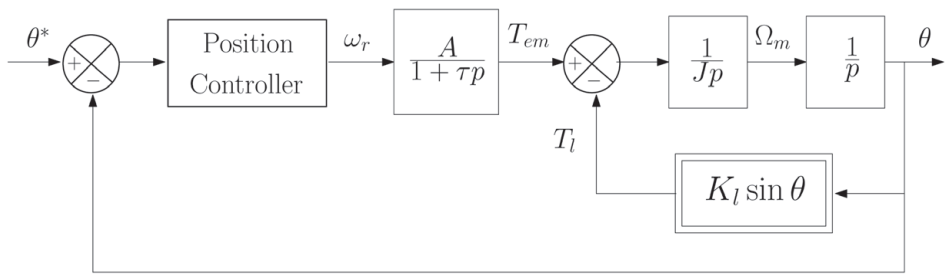
Figure 8.
Position control loop.

Then, we have:

$$
\begin{cases}
\dfrac{d\theta}{dt} = \Omega_m \\[3mm]
\dfrac{d^2\theta}{dt^2} = \dfrac{1}{J} T_{em} - \dfrac{K_l}{J} \sin\theta \\[3mm]
\dfrac{d^3\theta}{dt^3} = \dfrac{1}{J} \dfrac{dT_{em}}{dt} - \dfrac{K_l}{J} \dfrac{d\theta}{dt} \cos\theta
\end{cases}
\tag{7}
$$

This yields:

$$
\dfrac{d^3\theta}{dt^3} = \dfrac{1}{J} \left(-\dfrac{1}{\tau} T_{em} + \dfrac{A}{\tau} \omega_r \right) - \dfrac{K_l}{J} \dfrac{d\theta}{dt} \cos\theta
$$

$$
= -\dfrac{1}{\tau} \left(\dfrac{d^2\theta}{dt^2} + \dfrac{K_l}{J} \sin\theta \right) + \dfrac{A}{J\tau} \omega_r - \dfrac{K_l}{J} \dfrac{d\theta}{dt} \cos\theta
\tag{8}
$$

Thus, we can write:

$$
\dfrac{d^3\theta}{dt^3} + \dfrac{1}{\tau} \dfrac{d^2\theta}{dt^2} + \dfrac{K_l}{J} \dfrac{d\theta}{dt} + \dfrac{K_l}{J\tau} \theta + \varphi\left(\theta, \dfrac{d\theta}{dt}\right) = \dfrac{A}{J\tau} \omega_r
\tag{9}
$$

where:

$$
\varphi\left(\theta, \dfrac{d\theta}{dt}\right) = \dfrac{K_l}{J} \dfrac{d\theta}{dt} (\cos\theta - 1) + \dfrac{K_l}{J\tau} (\sin\theta - \theta) = 0\left(\theta, \dfrac{d\theta}{dt}\right)^3
\tag{10}
$$

For small values of θ, $\varphi\left(\theta, \frac{d\theta}{dt}\right)$ can be neglected, and then the mechanical part of the machine can be represented by a third order linear system described by the following transfer function:

$$
\dfrac{\theta}{\omega_r} = \dfrac{\dfrac{A}{J\tau}}{\left(p^2 + \dfrac{K}{J}\right)\left(p + \dfrac{1}{\tau}\right)}
\tag{11}
$$

It is to be noted that the application of the following nonlinear feedback represents a nonlinear compensator:

$$
\omega_{r'} = \omega_r - \dfrac{J\tau}{K_l} \varphi\left(\theta, \dfrac{d\theta}{dt}\right)
\tag{12}
$$

This loop realizes a feedback linearization. The transfer function between θ and ω_r' is expressed as:

$$
\dfrac{\theta}{\omega_r'} = \dfrac{\dfrac{A}{J\tau}}{\left(p^2 + \dfrac{K}{J}\right)\left(p + \dfrac{1}{\tau}\right)}
\tag{13}
$$

which is an exact transfer function without any approximation.

Observing this transfer function, it is clear that it contains two imaginary poles. This leads to a certain difficulty to control the system with a PID controller $C(p)$:

$$C(p) = K_c \left(1 + \frac{1}{T_i p} + T_d p \right) \qquad (14)$$

In fact, the system does not present any stability margin. Moreover, to have an adequate dynamical behavior, the derivative time constant (T_d) should be larger that the integral time constant (T_i), which is strongly not recommended.

3.4 DTC-SVM based position control scheme

The implementation scheme of a DTC-SVM based position regulation of an induction motor is shown in **Figure 9**. The idea is based on the decoupling between the amplitude and the argument of the stator flux reference vector.

The amplitude of this vector will be imposed equal to the nominal value of the stator flux, but the argument will be calculated according to the desired performances. In fact, the error between the reference position θ^* and the measured one θ is applied to the position regulator whose output provides the slip angular reference speed ω_r^*, which will be used to calculate the argument of the stator flux reference. Coordinates of the reference stator flux in the reference frame (α, β) are computed from its polar coordinates according to Eqs. (5). The coordinates of the reference voltage vector $v_{\alpha s}^*$ and $v_{\beta s}^*$ are determined using Eqs. (6).

Finally, the SVM block, which uses these later to generate the convenient stator voltages inverter in each modulation period, ensuring working with a constant commutation frequency.

Figure 9.
Induction motor position regulation based on the DTC-SVM strategy.

3.5 Concept of sliding mode DTC-SVM based position control

Sliding mode (SM) controllers perform well in non nonlinear systems than PI controllers [13, 14]. Indeed, the sliding mode control is a type of variable structure systems characterized by the high simplicity and the robustness against insensitivity to parameter variations and external disturbances [14–16]. Considering a nonlinear system described by the following state equation:

$$\dot{X} = f(X) + g(X)U \qquad (15)$$

A choice of the sliding surface $S(X)$ can be given by:

$$S(X) = h(X) - h(X^*) \qquad (16)$$

with X^* is a reference trajectory.

In order to decide a system trajectory, the equivalent control U_{eq} represents the required control to reach and to remain on the sliding surface. The corrected term ΔU is required to guarantee the remaining on the surface $S(X) = 0$.

Thus, one can choose for the controller the following expression:

$$U = U_{eq} + \Delta U \qquad (17)$$

The equivalent control can be designed as follows: when the system remains on the sliding surface, we have $S(X) = 0$, then $\dot{S}(X) = 0$. Since:

$$\dot{S}(X) = h_1(X)[f(X) + g(X)U] - h_1(X^*)\dot{X}^* = \mathcal{F}(X, X^*) + \mathcal{G}(X)U \qquad (18)$$

where $h_1(X) = \frac{dh}{dX}$.

This yields the following expression of the equivalent control:

$$U_{eq} = [h_1(X)g(X)]^{-1}\left[h_1(X^*)\dot{X}^* - h_1(X)f(X)\right] = -[\mathcal{G}(X)]^{-1}\mathcal{F}(X, X^*) \qquad (19)$$

under the regularity of matrix $\mathcal{G}(X) = [h_1(X)g(X)]$.

The term ΔU can be expressed as:

$$\Delta U = -U_0 \operatorname{sign}\left[\mathcal{G}^T(X)S(X)\right] \qquad (20)$$

In fact, if we consider the Lyapunov function:

$$V(X) = S^T S > 0 \qquad (21)$$

Its differential with respect to time is expressed as:

$$\dot{V} = S^T\dot{S} = S^T\mathcal{G}(X)\Delta U = -U_0 S^T \mathcal{G}(X)\operatorname{sign}\left[\mathcal{G}^T(X)S(X)\right] = -U_0\left\|\mathcal{G}^T(X)S(X)\right\|_1 \leq 0 \quad (22)$$

This yields that the closed loop system is stable.

3.5.1 Position sliding mode controller

The sliding surface is expressed as:

$$S_\theta = \left(\frac{d}{dt} + \lambda_1\right)^2 \varepsilon_\theta = 0 \qquad (23)$$

that is to say:

$$S_\theta = \frac{d^2\varepsilon_\theta}{dt^2} + 2\lambda_1\frac{d\varepsilon_\theta}{dt} + \lambda_1^2\varepsilon_\theta = 0 \tag{24}$$

with: $\varepsilon_\theta = \theta - \theta^*$. This choice takes into account that the error decreases exponentially after reaching the sliding surface. In fact, if $S_\theta = 0$, for $t \geq t_0$, we have:
$\varepsilon_\theta(t) = \{\varepsilon_\theta(t_0) + [\dot{\varepsilon}_\theta(t_0) + \lambda_1\varepsilon_\theta(t_0)](t - t_0)\}e^{-\lambda_1(t-t_0)}$.

In this case, function $h(X)$ is expressed as:

$$h(X) = \frac{1}{J}T_{em} + 2\lambda_1\Omega_m + \lambda_1^2\theta - \frac{K_l}{J}\sin\theta \tag{25}$$

To remain the state of the system on the sliding surface $S_\theta = 0$, we have: $\dot{S}_\theta = 0$. This leads to:

$$\dot{S}_\theta = \frac{d^3\varepsilon_\theta}{dt^3} + 2\lambda_1\frac{d^2\varepsilon_\theta}{dt^2} + \lambda_1^2\frac{d\varepsilon_\theta}{dt} = 0 \tag{26}$$

That is to say:

$$\dot{S}_\theta = \frac{1}{J}\left(-\frac{1}{\tau}T_{em} + \frac{A}{\tau}U\right) + 2\lambda_1\left(\frac{1}{J}T_{em} - \frac{K_l}{J}\sin\theta\right) + \left(\lambda_1^2 - \frac{K_l}{J}\cos\theta\right)\Omega_m - h_1(X^*)\dot{X}^*$$
$$= 0 \tag{27}$$

where:

$$h_1(X^*)\dot{X}^* = \left(\ddot{\Omega}_m^* + 2\lambda_1\dot{\Omega}_m^* + \lambda_1^2\dot{\theta}^*\right) \tag{28}$$

Then, it is easy to express the so-called equivalent control which corresponds to the required control remaining the system on the sliding surface:

$$U_{eq,\theta} = \frac{1}{A}T_{em} - 2\frac{\lambda_1\tau}{A}(T_{em} - K_l\sin\theta) - \frac{J\tau}{A}\lambda_1^2\Omega_m + \frac{\tau K_l}{A}\Omega_m\cos\theta + \frac{J\tau}{A}h_1(X^*)\dot{X}^* \tag{29}$$

Then, the slip angular reference speed ω_r can be expressed by:

$$\omega_r = U_{eq,\theta} - U_{0,\theta}\text{sign }(S_\theta) \tag{30}$$

The new structure of this control approach is given by the block diagram of **Figure 10**.

3.6 SM controllers with adaptive parameters estimation

If system (14) depends on an unknown parameter vector $\gamma = [\gamma_1\gamma_2 \ldots]^T$, the expression of the control depends on γ, that is to say: $U_{eq} = U_{eq}(\gamma)$ and the applied control law becomes:

$$\overline{U} = \overline{U}_{eq} + \Delta U \tag{31}$$
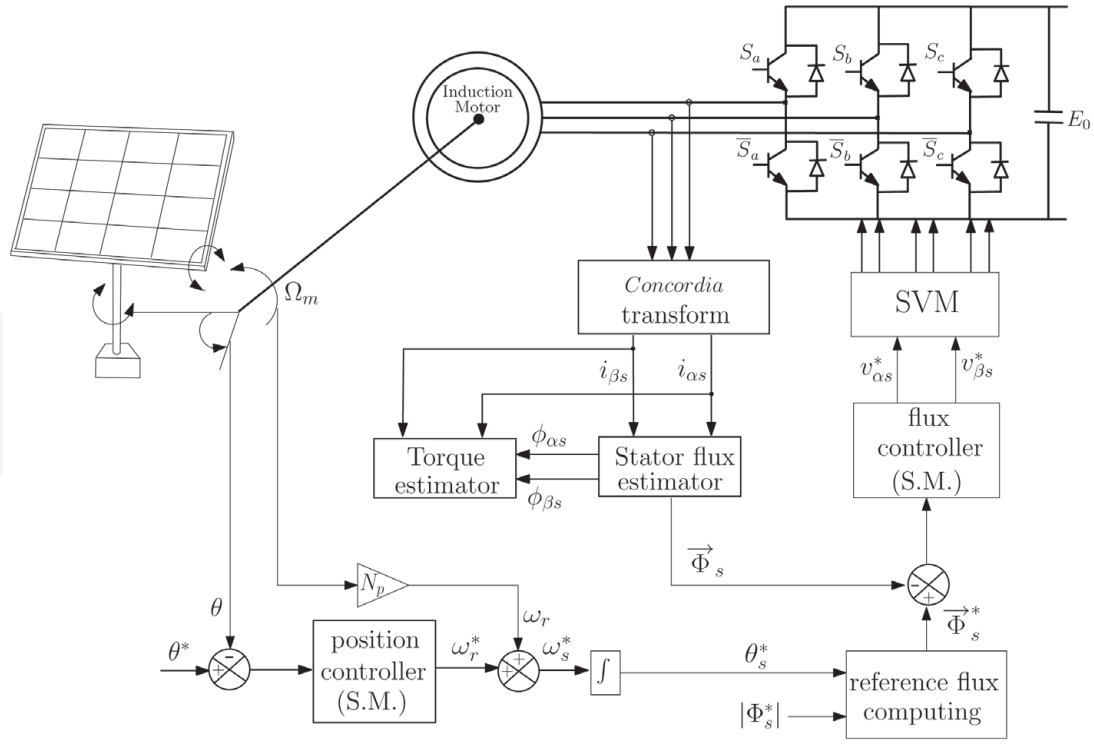
Figure 10.
Induction motor position regulation based on the DTC-SVM with sliding mode controllers.

where $\overline{U}_{eq} = U_{eq}(\overline{\gamma})$. $\overline{\gamma}$ is the estimated vector of γ.

Referring to Eq. (17), the differential of S is expressed as:

$$\dot{S} = \mathcal{F}(X, X^*) + \mathcal{G}(X)\overline{U} = \mathcal{F}(X, X^*) + \mathcal{G}(X)(\overline{U}_{eq} + \Delta U)$$

$$= \underbrace{\mathcal{F}(X, X^*) + \mathcal{G}(X)U_{eq}}_{=0} + \mathcal{G}(X)\Delta U + \mathcal{G}(X)(\overline{U}_{eq} - U_{eq})$$

$$= \mathcal{G}(X)\Delta U + \mathcal{G}(X)(\overline{U}_{eq} - U_{eq})$$

$$= \mathcal{G}(X)\Delta U + \mathcal{G}(X)(\overline{U}_{eq} - U_{eq}) + \underbrace{\left[\mathcal{G}(X) - \overline{\mathcal{G}}(X)\right]}_{=o(\Delta\gamma)} \underbrace{(\overline{U}_{eq} - U_{eq})}_{=o(\Delta\gamma)}$$

$$\underbrace{\qquad\qquad\qquad}_{=o(\Delta\gamma)^2}$$

$$= \mathcal{G}(X)\Delta U + \overline{\mathcal{G}}(X)\left(\Sigma_i \frac{\partial U_{eq}}{\partial\gamma_i}(\overline{\gamma})\Delta\gamma_i\right) + o(\Delta\gamma)^2$$

$$= \overline{\mathcal{G}}(X)\Delta U + \overline{\mathcal{G}}(X)\left(\Sigma_i \frac{\partial U_{eq}}{\partial\gamma_i}(\overline{\gamma})\Delta\gamma_i\right) + \left[\mathcal{G}(X) - \overline{\mathcal{G}}(X)\right]\Delta U + o(\Delta\gamma)^2$$

$$= \overline{\mathcal{G}}(X)\Delta U + \overline{\mathcal{G}}(X)\left(\Sigma_i \frac{\partial U_{eq}}{\partial\gamma_i}(\overline{\gamma})\Delta\gamma_i\right) + \left[\mathcal{G}(X) - \overline{\mathcal{G}}(X)\right]\Delta U + o(\Delta\gamma)^2$$

$$= \overline{\mathcal{G}}(X)\Delta U + \left(\sum_i\left[\overline{\mathcal{G}}(X)\frac{\partial U_{eq}}{\partial\gamma_i}(\overline{\gamma}) + \frac{\partial\mathcal{G}(X)}{\partial\gamma_i}\Delta U\right]\Delta\gamma_i\right) + o(\Delta\gamma)^2$$

$$(32)$$

with $\Delta\gamma = \overline{\gamma} - \gamma$ and $\overline{\mathcal{G}}(X)$ is the expression of $\mathcal{G}(X)$ for $\gamma = \overline{\gamma}$.

• Theorem

Control laws (17), (19) and (20) stabilize system (15) with the following adaptive laws:

$$\dot{\overline{\gamma}}_i = -\eta_i S^T \left(\overline{G}(X) \frac{\partial U_{eq}}{\partial \gamma_i}(\overline{\gamma}) + \frac{\partial G(X)}{\partial \gamma_i} \Delta U \right) \tag{33}$$

• Proof

Let us consider the following Lyapunov function:

$$V = \frac{1}{2} S^T S + \frac{1}{2} \sum_i \frac{1}{\eta_i} \Delta \gamma_i^2 \tag{34}$$

In the following, it assumed that vector γ is constant or it has slow variations with respect to time, in such away that we can neglect its differential with. respect to time: $\dot{\gamma} \simeq 0$. Then, we can write: $\Delta\dot{\gamma} \simeq \dot{\overline{\gamma}}$.
The differential with respect to time of function V is expressed as:

$$\dot{V} = s^T \dot{S} + \Sigma_i \frac{1}{\eta_i} \Delta\gamma_i \Delta\dot{\gamma}_i$$

$$= S^T \left[\overline{G}(X)\Delta U + \left(\Sigma_i \left[\overline{G}(X) \frac{\partial U_{eq}}{\partial\gamma_i}(\overline{\gamma}) + \frac{\partial g(X)}{\partial\gamma_i}\Delta U \right] \Delta\gamma_i \right) + o(\Delta\gamma)^2 \right]$$

$$+ \Sigma_i \frac{1}{\eta_i} \Delta\gamma_i \Delta\dot{\gamma}_i + o(\Delta\gamma)^2$$

$$= S^T \overline{G}(X)\Delta U + \Sigma_i \underbrace{\left[S^T \left(\overline{G}(X)\frac{\partial U_{eq}}{\partial\gamma_i}(\overline{\gamma}) + \frac{\partial G(X)}{\partial\gamma_i}\Delta U \right) + \frac{1}{\eta_i}\Delta\dot{\gamma}_i \right]}_{=0} \Delta\gamma_i + o(\Delta\gamma)^2 \tag{35}$$

$$= S^T \overline{G}(X)\Delta U + o(\Delta\gamma)^2 = -S^T \overline{G}(X) \, \mathrm{sign}\left[\overline{G}^T(X)S(X) \right] + o(\Delta\gamma)^2$$

$$= - \left\| \overline{G}^\tau(X)S(X) \right\|_1 + o(\Delta\gamma)^2 \leq 0$$

where $\|\cdot\|_1$ is the norm "1" of a vector which corresponds to the sum of absolute values of its components.

3.6.1 Position adaptive SM controller with variations on the mutual inductance and the rotor resistance

The sensitivity of the DTC-SVM to (i) variations on the magnetic permeability of the stator and rotor cores, and (ii) variations on the rotor resistance, which can vary with time and operating conditions, can be removed by an online estimation of the mutual inductance and the rotor resistance. The adaptive SM of the speed can be derived based on the mutual inductance and rotor resistance estimations using the *Lyapunov* theorem [17].
It is easy to show that:

$$U_\theta = \overline{U}_{eq,\theta} - U_{0,\theta} \, \mathrm{sign}\,(S_\Omega) \tag{36}$$

where:

$$\overline{U}_{eq,\theta} = -\left[\overline{\mathcal{G}}(X)\right]^{-1}\overline{\mathcal{F}}(X,X^*) \tag{37}$$

Then:

$$\dot{S}_\theta = \mathcal{F}(X,X^*) + \mathcal{G}(X)\overline{U}_\theta = \mathcal{F}(X,X^*) + \mathcal{G}(X)\left(\overline{U}_{eq,\theta} + \Delta U_\theta\right)$$

$$= \mathcal{F}(X,X^*) + \mathcal{G}(X)U_{eq,\theta} + \mathcal{G}(X)\Delta U_\theta + \mathcal{G}(X)\left(\overline{U}_{eq,\theta} - U_{eq,\theta}\right) \tag{38}$$

$$= \mathcal{G}(X)\Delta U_\theta + \mathcal{G}(X)\left(\overline{U}_{eq,\theta} - U_{eq,\theta}\right)$$

• Corollary

The following slip angular reference speed control law stabilizes the speed loop:

$$\omega_r = \overline{U}_{eq,\theta} - U_{0,\theta}\,\text{sign}\,\,(S_\Omega) \tag{39}$$

where $\overline{U}_{eq,\theta} = U_{eq,\theta}(\overline{M},\overline{R}_r)$, $\overline{M}$ and $\overline{R}_r$ are estimator values of the mutual inductance and the rotor resistance given by the following updating laws:

$$\dot{\overline{M}} = -\eta_{\theta_1}\overline{G}S_\theta\left(\frac{\partial U_{eq,\theta}}{\partial M}\right)$$

$$\dot{\overline{R}}_r = -\eta_{\theta_2}\overline{G}S_\theta\left(\frac{\partial U_{eq,\theta}}{\partial R}\right) \tag{40}$$

with: η_{θ_1} and η_{θ_2} positive scalars, $G = G(M,R_r)$ and $\overline{G} = \overline{G}(\overline{M},\overline{R}_r)$ defined in Eq. (17).

• Proof

Considering the following function:

$$V_\theta = \frac{1}{2}S_\theta^2 + \frac{1}{2\eta_{\theta_1}}\Delta M^2 + \frac{1}{2\eta_{\theta_2}}\Delta R_r^2 \tag{41}$$

with $\Delta M = \overline{M} - M$ and $\Delta R_r = \overline{R}_r - R_r$.
The time derivative of the *Lyapunov* function can be expressed as:

$$\dot{V}_\theta = S_\theta\dot{S}_\theta + \frac{1}{\eta_{\theta_1}}\Delta M\Delta\dot{M} + \frac{1}{\eta_{\theta_2}}\Delta R_r\Delta\dot{R}_r \tag{42}$$

However:

$$\overline{U}_{eq,\theta} - U_{eq,\theta} = (\overline{M} - M)\left(\frac{\partial U_{eq,\theta}}{\partial M}\right) + (\overline{R}_r - R_r)\left(\frac{\partial U_{eq,\theta}}{\partial R_r}\right) + o(\Delta M,\,\,\Delta R_r)^2 \tag{43}$$

Moreover:

$$\mathcal{G}\,\,(\overline{U}_{eq,\theta} - U_{eq,\theta}) = \overline{\mathcal{G}}(\overline{U}_{eq,\theta} - U_{eq,\theta}) + o(\Delta M,\,\,\Delta R_r)^2 \tag{44}$$

Thereby, Eq. (42) gives:

$$\dot{V}_\theta = -U_{0,\theta} \mathcal{G}(X)|S_\Omega| + \Delta M \underbrace{\left[\overline{\mathcal{G}} \left(\frac{\partial U_{eq,\theta}}{\partial M} \right) + \frac{1}{\eta_{\theta_1}} \Delta \dot{M} \right]}_{=0}$$

$$+ \Delta R_r \underbrace{\left[\overline{\mathcal{G}} \left(\frac{\partial U_{eq,\theta}}{\partial R_r} \right) + \frac{1}{\eta_{\theta_2}} \Delta \dot{R}_r \right]}_{=0} + o(\Delta M, \Delta R_r)^2 \qquad (45)$$

$$= -U_{0,\theta} \mathcal{G}(X)|S_\Omega| + o(\Delta M, \ \Delta R_r)^2 \leq 0$$

Since $\mathcal{G}(X) > 0$, $\dot{V}_\theta$ is negative. Then, the system is stable.

3.7 Simulation results investigated SM DTC-SVM approach based position control

Simulation works have been carried out in order to investigate performances of the position control of the induction motor drive under the above-presented DTC-SVM strategies, using PID, PID with a nonlinear compensator and SM controllers. For the sake of comparison, both strategies have been considered in the same induction motor drive using the same implementation conditions, such that:

- a reference stator flux Φ_s^* equal to 1 Wb,

- The modulation period has been fixed to $T_{mod} = 150\mu s$ in all DTC-SVM approaches under study,

- Constants involved in the position SM controller are: $U_{0,\theta} = 50$ and $\lambda_\theta = 100$. The constants involved in the flux SM controller are: $U_{0,\phi}, = 150$ and $\lambda_\phi = 2$.

The desired trajectory is defined by smooth variations of the position θ, the speed Ω_m and the torque C_{em}, leading to:

- variations of θ form $-60°$ (morning panel position) to $30°$ from 0 s to 1 s,

- constant value of θ equal to $30°$ from 1 s to 1.5 s.

- variations of θ form $30°$ to $60°$ (afternoon panel position) from 1.5 s to 2.5 s,

- constant value of θ equal to $60°$ from 2.5 s to 4 s.

The analysis of simulation results leads to the following items:

- **Figures 11** and **12** present evolutions of the position θ, the speed Ω_m, the torque C_{em}, the flux $|\Phi_s|$ and the current i_{as}, using PID controllers (figures indexed by 1), PID controllers with a nonlinear compensator (figures indexed by 2), and SM controllers (figures indexed by 3). It is well obvious that a good tracking has been realized by these control approaches. It is also obvious, that there is no significant difference between results yielded by PID controllers and PID controllers with a nonlinear compensator. This justifies that the nonlinear term $\varphi\left(\theta, \frac{d\theta}{dt}\right)$ can be neglected. Moreover, ripples of the torque, the flux and stator currents are smallest for results given by SM controllers.
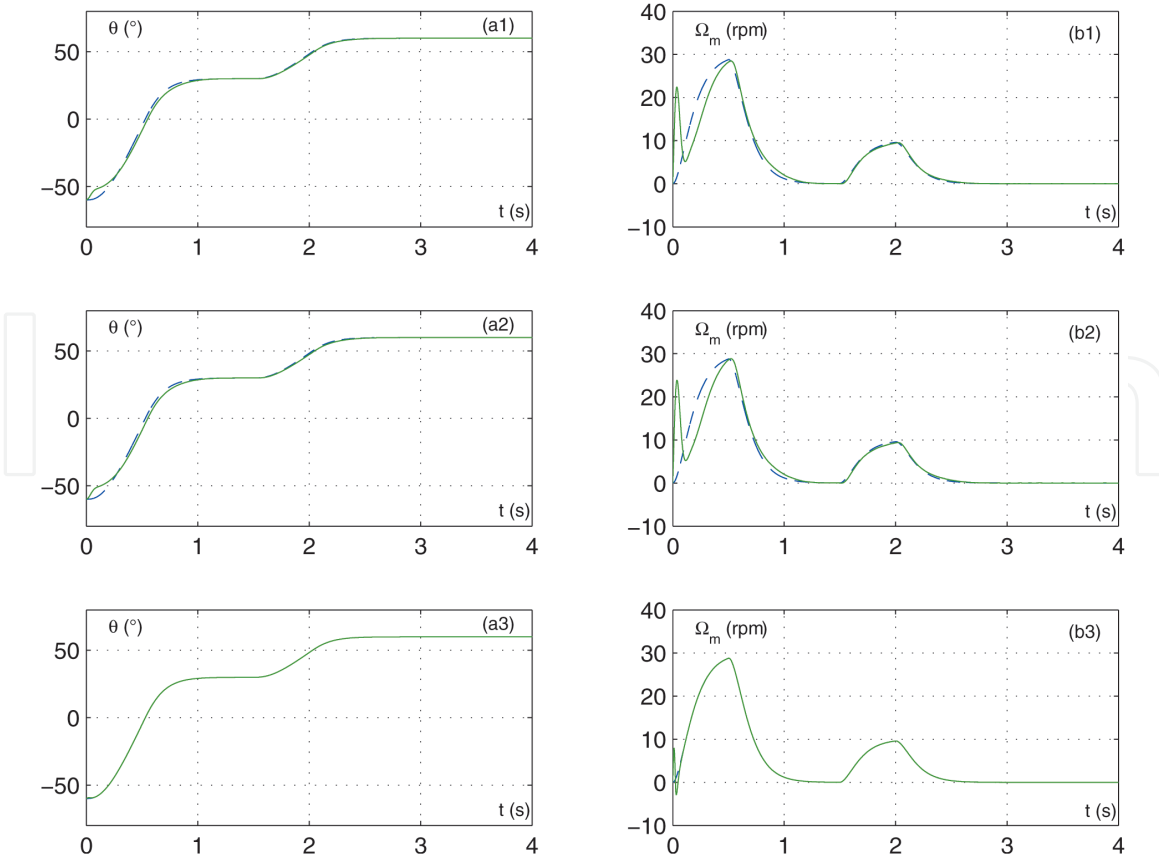
Figure 11.
Induction motor position regulation considering (subscript "1") DTC-SVM approach using PI controller, (subscript "2") DTC-SVM approach using PI controller with a nonlinear compensator and (subscript "3") DTC-SVM approach using sliding mode controllers. Legend: (a) evolution of the position and its reference and (b) the speed of the motor and its reference.

- **Figures 13** and **14** present the same variable evolutions for variations of machine parameters as: $+100\%$ variations on the stator resistance R_s, $+100\%$ variations on the rotor resistance R_r and -50% variations on the mutual inductance M. It is clear that results, yielded from PID controllers without and with a nonlinear compensator, present important oscillations. However, SM controllers with parameter's updating give same results as in the case where parameters are known and do not vary.

- Thus, the implementation of the DTC-SVM using sliding mode controllers strategies highlights high dynamical performances obtained with the lowest torque ripple, the lowest flux ripple and the lowest current ripple.

3.8 Performance criteria

Considering the same simulation, we propose to use performance criteria defined in the appendix.

In the following, the steady state operating point is defined by a desired position θ equal to 60° for the time larger than 2.5 s.

- Total Harmonic Distortion (THD)

The first criterion is the average total harmonic distortion (THD) of the stator current which is defined in the Appendix.
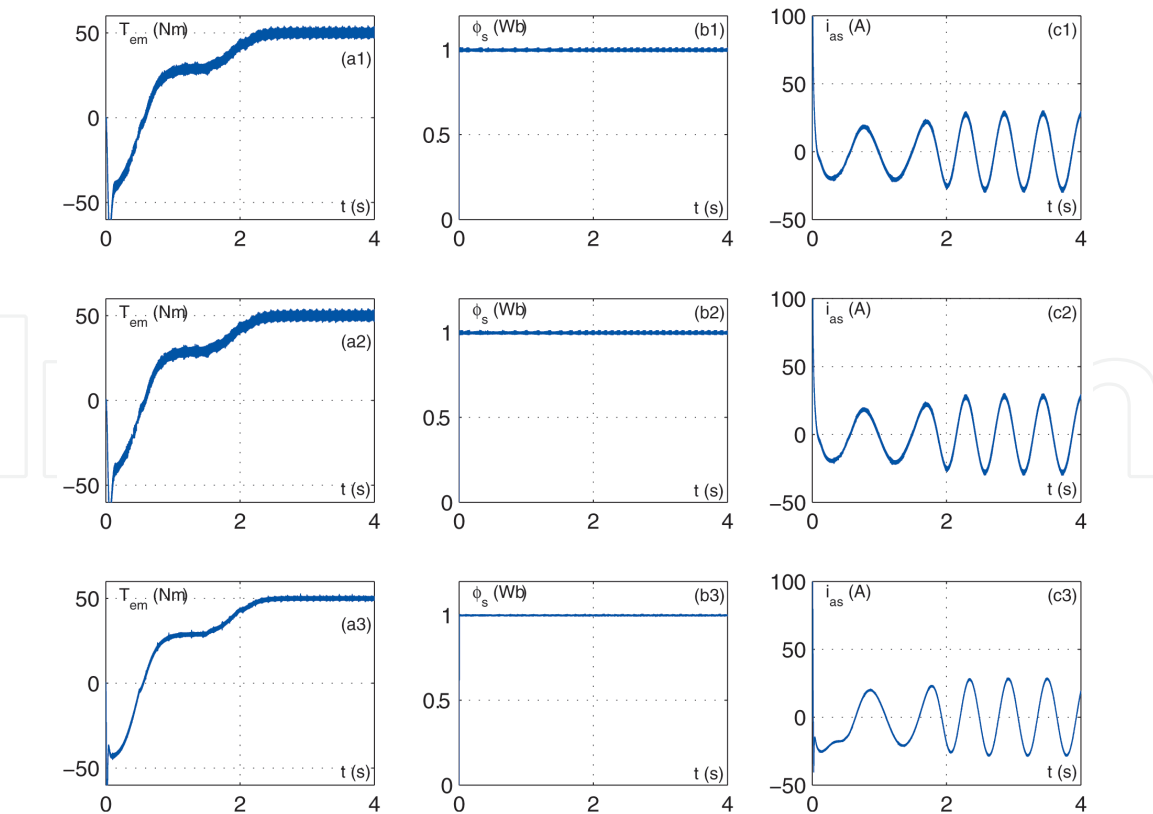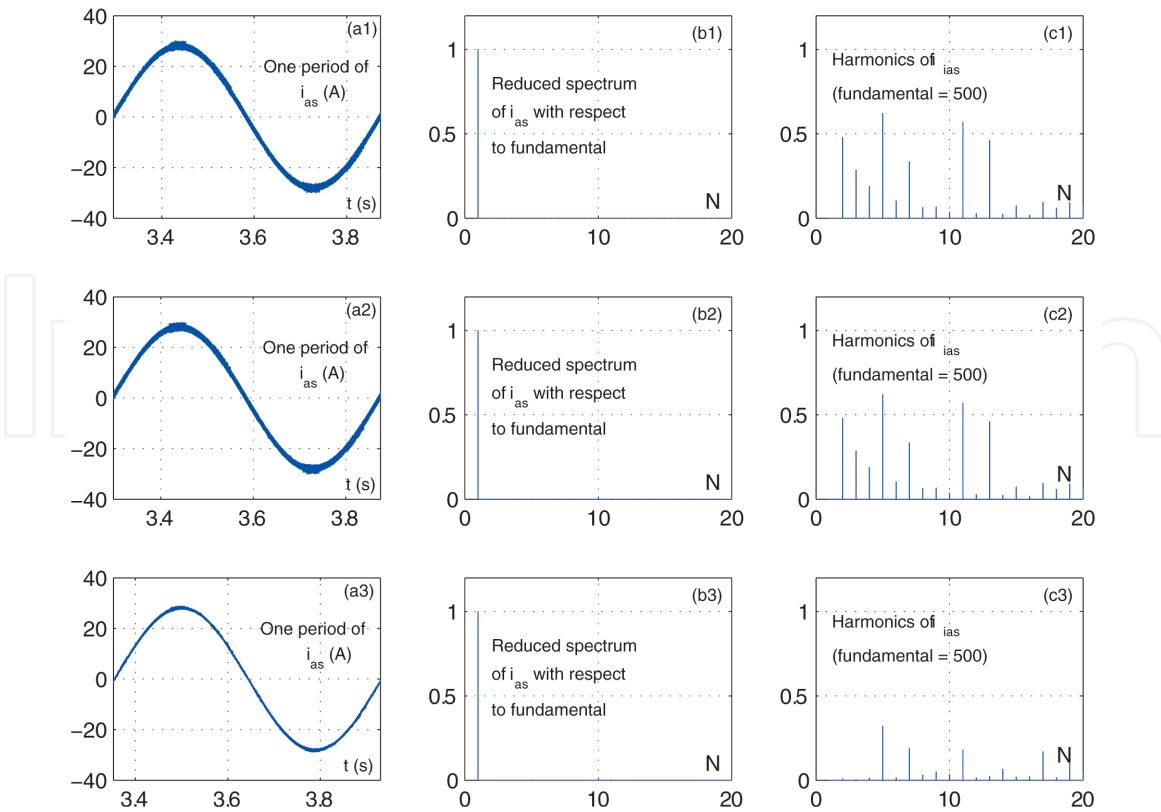
Figure 12.
Induction motor position regulation considering (1) DTC-SVM approach using PI controller, (2) DTC-SVM approach using PI controller with a nonlinear compensator and (3) DTC-SVM approach using sliding mode controllers. Legend: (a) evolution of the electromagnetic torque, (b) the stator flux and (c) the stator current of phase a.
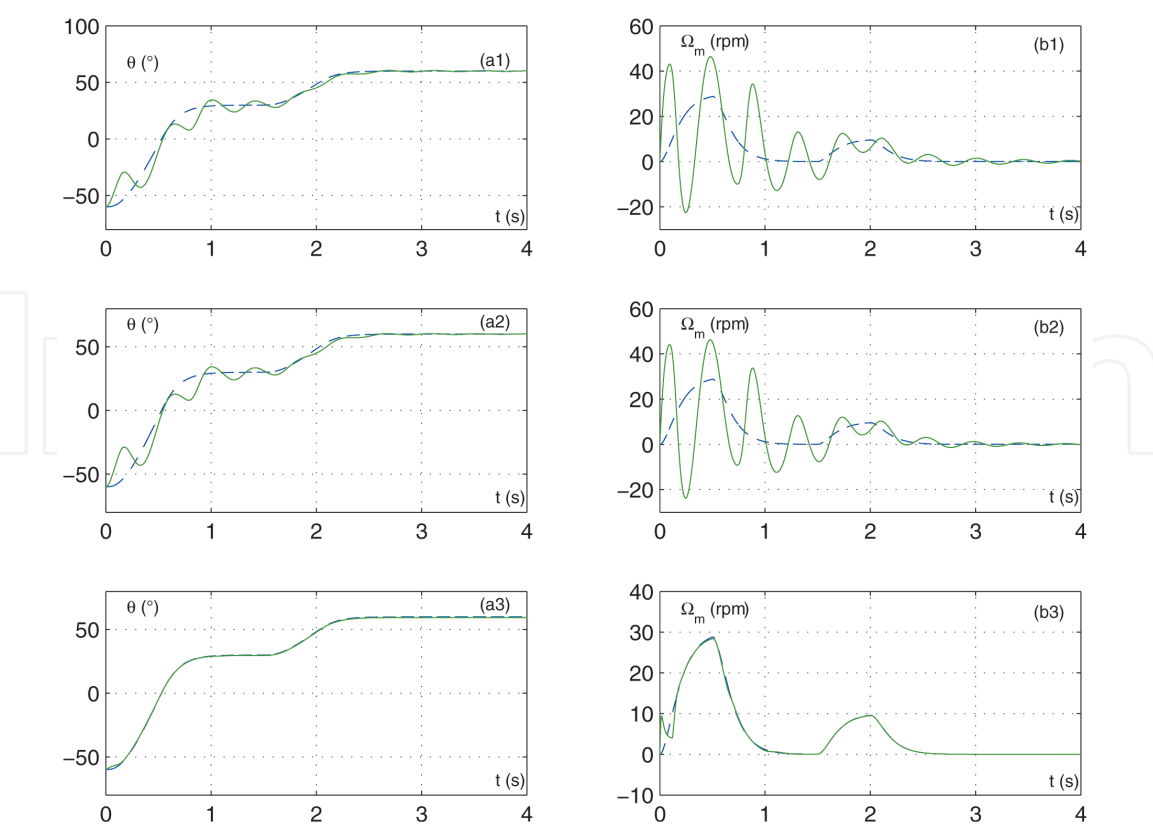
Figure 13.
Induction motor position regulation, considering +100% variations on the stator resistance, (1) DTC-SVM approach using PI controller, (2) DTC-SVM approach using PI controller with a nonlinear compensator and (3) DTC-SVM approach using sliding mode controllers. Legend: (a) evolution of the position and its reference and (b) the speed of the motor and its reference.
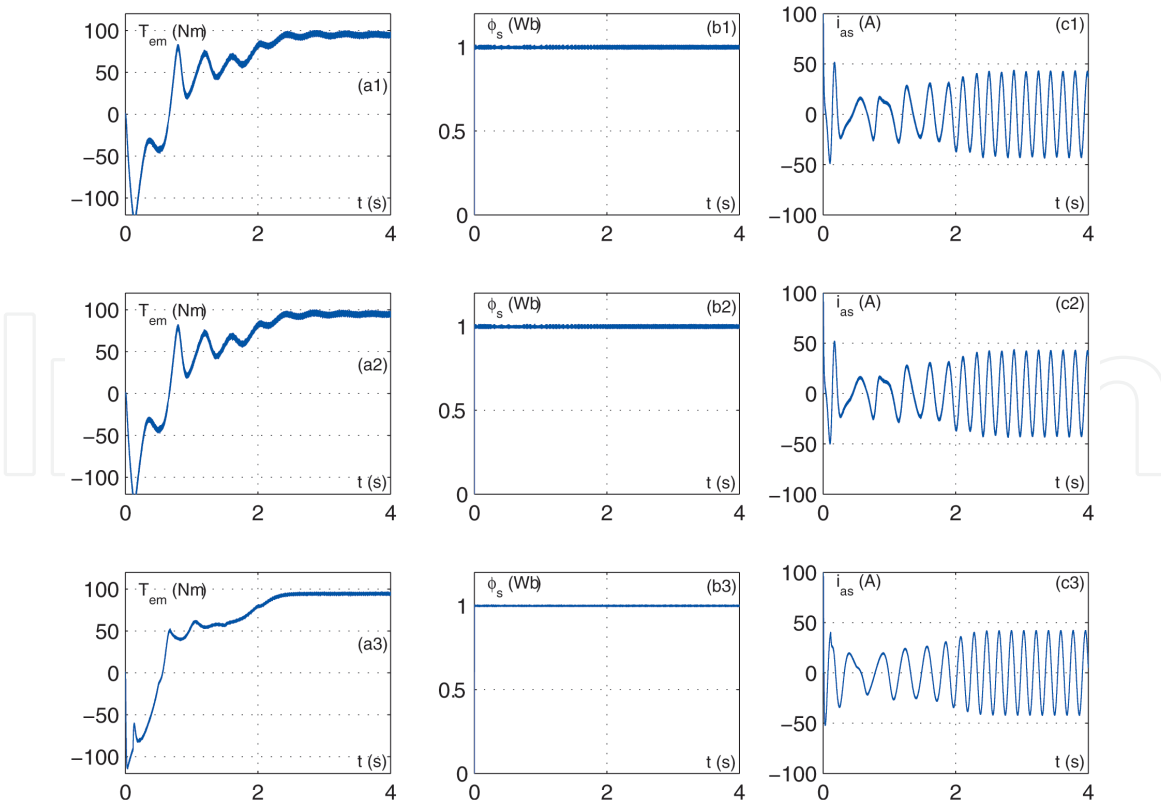
Figure 14.
Induction motor position regulation, considering +100% variations on the stator resistance, considering (1) DTC-SVM approach using PI controller, (2) DTC-SVM approach using PI controller with a nonlinear compensator and (3) DTC-SVM approach using sliding mode controllers. Legend: (a) evolution of the electromagnetic torque, (b) the stator flux and (c) the stator current of phase a.

Figure 15.
Spectrum of the current i_{as}. (a) Normalized spectrum, (b) higher harmonics of the spectrum current (c) one period of the current i_{as}. (subscript "1") DTC-SVM approach using PI controller, (subscript "2") DTC-SVM approach using PI controller with a nonlinear compensator and (subscript "3") DTC-SVM approach using sliding mode controllers.

	PI without a NL compensator	PI with a NL Compensator	Sliding Mode Controllers
THD (%)	3.07	3.07	1.23

Table 4.
*Total harmonic distortion of the stator current i_{as}.*

In this context, the frequency spectrum of the stator current i_{as} has been analyzed by the observation of amplitudes of all its harmonics frequencies. **Figure 15** shows the evolution of one period of i_{as} between 3 s and 4 s, its spectrum (only 20 harmonics has been presented). It is obvious that SM controllers give less ripples of the stator current.

The total harmonic distorsion criterion of the stator current i_{as} is given by **Table 4** which shows that SM controllers give the lowest criterion.

• Ratio of torque and flux ripples.

The second comparison criterion translates the torque and the flux ripples around their steady state values $|\Phi_s| = 1$ and $T_{em,mean} = K_l \sin \frac{\pi}{6}$.

Figure 16 presents the evolution of the torque T_{em} and the flux $|\Phi_s|$ from 3 s to 4 s. Computations of flux ripple criteria are given by **Table 5**, and computations of torque ripple criteria are given by **Table 6**. These tables confirm that the PID controllers without a nonlinear compensator and PID controllers with a nonlinear compensator give same results. However, SM controllers give less ripples of the flux and the torque.
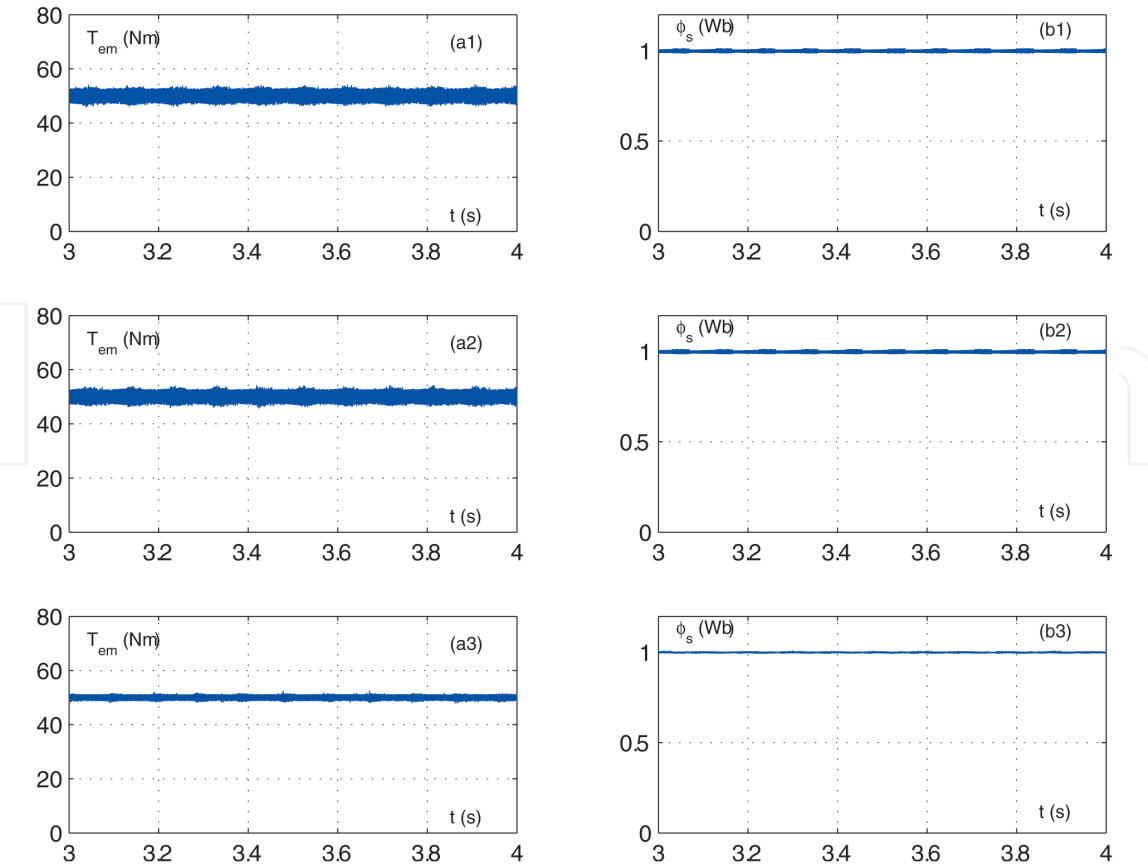
Figure 16.
Zoomed shapes of (a) electromagnetic torque and (b) stator flux. In the case of (subscript "1") DTC-SVM approach using PI controller, (subscript "2") DTC-SVM approach using PI controller with a nonlinear compensator and (subscript "3") DTC-SVM approach using sliding mode controllers.

	PI without a NL compensator	PI with a NL Compensator	Sliding Mode Controllers
$\Phi_{RIP,1}$ (%)	0.38	0.38	0.12
$\Phi_{RIP,2}$ (%)	0.44	0.44	0.15
$\Phi_{RIP,\infty}$ (%)	1.26	1.33	0.65

Table 5.
Flux ripple criteria.

	PI without a NL compensator	PI with a NL Compensator	Sliding Mode Controllers
$T_{RIP,1}$ (%)	1.88	1.86	0.92
$T_{RIP,2}$ (%)	2.71	2.66	0.62
$T_{RIP,\infty}$ (%)	8.17	8.34	4.65

Table 6.
Torque ripple criteria.

4. Conclusion

In this chapter, the DTC position control of induction motor controlling photo-voltaic panel has been considered. This panel is commonly exposed to the sun in fixed positions corresponding to the maximum sunshine recorded during a day. Firstly, the DTC-SVM approach using hysteresis controllers has been compared to the basic DTC strategy and DTC strategy with a look-up table including only active voltage vectors. Then, the problem of position regulation of an IM under DTC-SVM approaches has been treated. In fact, a comparison between three DTC-SVM approaches: a DTC-SVM approach using PI controllers, a DTC-SVM approach using PI controllers with a nonlinear compensator, and a DTC-SVM approach using sliding mode controllers, has been proposed. Finally, an adaptation approach of parameter estimators has been implemented in order to eliminate the effects of parameter variations and load disturbances. It has been shown through simulations the sliding mode DTC-SVM approach (i) eliminates the demagnetization effects, and gives lowest ripples on the torque and on the flux, (ii) presents less harmonic distortion on the stator currents, and (iii) it presents good performances with a good robustness with respect to parameter's variations and load disturbances, particularly in the case of adapted estimators of machine parameters.

Author details

Fatma Ben Salem
Control and Energy Management Laboratory (CEMLab), University of Sfax, Sfax
Engineering School, BP 1173, 3038 Sfax, Tunisia

*Address all correspondence to: fatma.bensalem@isgis.usf.tn; fatma_bs@yahoo.fr

IntechOpen

References

[1] Takahashi., I., and Ohmori, Y., High Performance Direct Torque Control of Induction Machine. IEEE Power Electronics Specialists Conf. (PESC'88), 2:870–876, Kyoto-Japan, April 1988.

[2] Depenbrock, M., 'Direct Self-Control (DSC) of Inverter-Fed Induction Machine'. *IEEE Trans. Industry Applications,* 28(3):581–588, May-juin 1992.

[3] Ben Salem, F., and Feki, M., (2019) 'An improved DTC of Induction Motor for Electric Vehicle Propulsion: An Intent to Provide Comfortable Ride', *from book: Optimization of Green Transportation Problems: Fundamentals and Applications,* Wiley, December 16, 2019.

[4] El Ouanjli, N., Derouich, A., El Ghzizal, A., Motahhir, S., Chebabhi, A., El Mourabit, Y., and Taoussi, M., (2019) 'Modern improvement techniques of direct torque control for induction motor drives - a review', *Protection and Control of Modern Power Systems,* 4(11): 12 pages.

[5] Bouzidi, B., Ben Salem, F., Yangui, A., and Masmoudi,A., (2007) 'Direct Torque Control strategy Based Maximum Sunshine Position Tracking', *Second International Conference and Exhibition on Ecological Vehicles and Renewable Energies* (EVER'07), Monte Carlo-Monaco, March–April 2007.

[6] Bouzidi, B., Ben Salem, F., and Yangui, A., (2008) 'The Classical and Analytic DTC for Photovoltaic Panel Position and Control', *International Journal of Sciences and Techniques of Automatic Control and Computing Engineering* (IJ-STA), special issue CEM, 636–651.

[7] Davari, S. A., Hasankhan, E. and haburi, D. A. (2011) 'A comparative study of DTC-SVM with three-level inverter and an improved predictive torque control using two-level inverter', *2nd Power Electronics, Drive Systems and Technologies Conference,* Tehran, Iran.

[8] Zhifeng, Z., Renyuyan,T., Boadong, B. and Dexin, X. (2010) 'Direct torque control based on space vector modulation with adaptive stator flux observer for induction motors', *IEEE Trans. Magnetics,* Vol. 48, No. 8, pp.3133–3136.

[9] Meroufel, A., Wira, P., Nefsi, M. and Massoum, A. (2012) 'Contle directe du couple de la machine asynchrone bas sur MLI vectorielle discrtise (DSVM-DTC)', *Acta Electrotehnica*, Vol. 1, pp.35–40.

[10] Abu-Rub, H., Stando, D. and Kazmierkowski, M.P. (2013) 'Simple speed sensorless DTC-SVM scheme for induction motor drives', *Bulletin of the Polish Academy of Sciences Technical Sciences,* Vol. 61, No. 2, pp.301–307.

[11] Manuel, A. and Francis, J. (2013)'Simulation of direct torque controlled induction motor drive by using space vector pulse width modulation for torque ripple reduction', *International Journal of Advanced Research in Electrical, Electronics and Instrumentation Engineering*, Vol. 2, No. 9, pp.4471–4478.

[12] Bendaikha, A., Saad, S., Abdou, A., Defdaf, M., Laamari Y., (2019) 'A Study of SVM-DTC and Conventional DTC for Induction Motors Drive Fed by Five-level Inverter', *European Journal of Electrical Engineering,* Vol. 21, No. 1, pp.85–91.

[13] Ben Salem,F., Bahri,I., Maamri,H. and Derbel,N. A Second-Order Sliding Mode Control of Switched Reluctance Motor, J. of Power and Energy Systems, 2020, doi.org/10.1080/15325008.2020.1797937, pp. 640–651.

[14] Ben Salem,F. and Derbel N., Direct torque control of induction motors based on discrete space vector modulation using adaptive sliding mode control, Int. J. of Electric Power Components and Systems, 2014, 42, (14), pp. 1598–1610.

[15] Ben Salem,F. and Derbel,N., A Sliding Mode field Oriented Control of an Induction Machine Operating with Variable Parameters, J. of Power and Energy Systems, 2007, 27,(2), pp. 205212.

[16] Ben Salem,F. and Derbel,N., DTC-SVM-Based Sliding Mode Controllers with Load Torque Estimators for Induction Motor Drives, Chapter 14 of the Book: Applications of Sliding Mode Control, Studies in Systems, Decision and Control 79, Springer Science +Business Media Singapore 2017, pp. 269297.

[17] F. Ben Salem and N. Derbel, "Position Control Performance Improvement of DTC-SVM for an Induction Motor: Application to Photovoltaic Panel Position", *International Journal of Renewable Energy Research (IJRER)*, 4(4):879–892, 2014.